

## PERFORATED NANOANTENNA REFLECTARRAY

Saber H. Zainud-Deen<sup>1</sup>, Hend A. El-Azem Malhat<sup>1, \*</sup>,  
Shaymaa M. Gaber<sup>2</sup>, and Kamal H. Awadalla<sup>1</sup>

<sup>1</sup>Faculty of Electronic Eng., Menoufia University, Egypt

<sup>2</sup>Egyptian Russian University, Egypt

**Abstract**—This paper presents a design of perforated nanoantenna reflectarray. The use of metallic nanostructures made of Silver and/or Gold at appropriate wavelength cause fascinating unusual electromagnetic effects. Reflectarray consists of an array of unit cell made from Silver is investigated. The effect of the number of perforated holes in the unit cell configurations is investigated for proper reflection coefficient phase compensation. A linearly polarized pyramidal nano-horn is used to feed the perforated nanoantenna reflectarray. The radiation characteristics of  $9 \times 9$  perforated nanoantenna reflectarray are illustrated. A high gain of 20.5 dB is obtained at the designed frequency of 735 THz. A comparison between solid Silver sheet with no perforation holes and the proposed perforated reflectarray is explained.

### 1. INTRODUCTION

Reflectarray antennas have received considerable attention over the years and are quickly finding many applications. Reflectarray antennas combine the same features of parabolic reflectors and phased arrays providing a directive beam in a desired scanned angle. The most important advantages of reflectarrays over phased arrays are the elimination of complexity and losses of the feeding network and the higher efficiency [1–4]. The reflectarray consists of an array of unit-cells illuminated by a primary feed. Each unit-cell is designed in such a way to correct the phase of the incident wave as is done in the traditional parabolic reflector. In reflectarrays, the phase of the reflected field from each element is adjusted so that the main beam can be directed to a desired direction. Several reflectarray approaches

---

*Received 11 January 2013, Accepted 8 March 2013, Scheduled 12 March 2013*

\* Corresponding author: Hend Abd El-Azem Malhat (er\_honida1@yahoo.com).

are proposed to control the reflection phase in the literature [5]. For example, one is to use identical microstrip patches with different-length phase-delay lines attached so that they can compensate for the phase delays over the different paths from the illuminating feed. The other is to use variable-size patches, dipoles, or rings so that elements can have different scattering impedances and, thus, different phases to compensate for the different feed-path delays. To overcome the shortcoming of narrow bandwidth of the reflectarray, dual-band multi-layer reflectarrays using variable patch size, annular rings, and crossed dipoles are being developed [6–8].

Generally, conventional antennas act as a source and transformer of electromagnetic (EM) radiation at radio frequencies (RF) and microwaves, resulting in their sizes being comparable with the operational wavelength. Recent success in the fabrication of nanoscale elements allows bringing the concept of the RF antennas to optics, leading to the development of optical nanoantennas [9]. Nanoantennas are metal nanostructures used to enhance, confine, receive, and transmit optical fields [10]. Nanoantenna is one of the most developing in plasmonics due to their ability to overcome the size and impedance mismatch between subwavelength emitters and free space radiation [11]. The ability to redirect propagating radiation and transfer it into localized subwavelength modes at the nanoscale makes the optical nanoantennas highly desirable for many applications. Several applications of nanoantennas have been used such as spectroscopy and high resolution near-field microscopy [9], subwavelength light confinement and enhancement [12], photovoltaic [13], sensing [14], molecular response enhancement [15], non-classical light emission [16], and communication [17]. Different nanoantennas have been investigated in the literature. By far, research in this nanoantennas field has utilized the coinage metals, Gold, Copper, and Silver, yet many potential commercial applications would be optimally realized by inexpensive plasmonic materials compatible with either high-technology or high-throughput manufacturing methods. Recently, a method of realizing nanoantennas reflectarray system at optical frequencies by using nanoparticles of concentric structures with cores made of ordinary dielectrics and shell of plasmonic materials has been suggested in [18]. The scattering resonance of these concentric structures can be tailored at different wavelength range by adjusting the core and shell radii or the material properties. Later, the perforated technique was used in the dielectric Fresnel lens design to obtain proper phase compensation and gain enhancement [19]. The technique of perforating a dielectric sheet eliminates the need to position and bond individual elements in an

array. Perforations create different effective dielectric permittivity and make the fabrication of the arrays feasible. The array is made from one piece of material; and inserting air holes with defined diameters and spacing in the required position. The perforations result in lowering the effective dielectric constant for the substrate at the region of air holes. The finite-integration technique, FIT [20] is used to calculate the characteristics of the reflectarray nanoantenna.

In this paper, the radiation characteristics of perforated nanoantennas reflectarray are calculated. The paper is organized as follows. Section 2 describes basic material properties used in designing nanoantennas. Section 3 offers the complete description of the design of nanoantenna reflectarray unit cell and its designing parameters. Finally, in Section 3 conclusions are drawn.

## 2. THEORY

Generally, the reflectarray transforms the spherical wave emanating from the feed into a plane wave at the output, like conventional parabolic reflector antenna. The array is located in the  $x$ - $y$  plane and is illuminated by a feed nano-horn. A required phase distribution,  $\varphi_i(x_i, y_i)$ , at each element of the array is needed to collimate a beam in the  $(\theta_o, \varphi_o)$  direction and is determined by

$$\varphi_i(x_i, y_i) = k_o(d_i - \sin \theta_o(x_i \cos \varphi_o + y_i \sin \varphi_o)) \quad (1)$$

$$d_i = \sqrt{(x_i - x_f)^2 + (y_i - y_f)^2 + (z_f)^2} \quad (2)$$

where  $k_o$  is the propagation constant in vacuum,  $d_i$  is the distance from the feed nanohorn  $(x_f, y_f, z_f)$  to the element  $i$  of the array and  $(x_i, y_i)$  are the coordinates of the cell element  $i$ . The phase shift of each cell element in the reflectarray should be between  $0$  and  $360^\circ$ . The use of metallic nanostructures made of Silver and/or Gold may become promising. The light illumination of such metals at appropriate wavelength may cause fascinating unusual electromagnetic effects [21] leading to promising applications for optical telecommunication, integrated optics and optical sensors. Most of these effects appear due to an excitation of Surface Plasmon Polariton (SPP) resonances. Due to high losses at optical frequencies, the assumption of perfect electrical conductor is no longer valid. The dielectric function of material substrate, used in nanoantennas, have been derived by fitting a Drude model given by [18]

$$\varepsilon = \varepsilon_0 \left[ 1 - \frac{\omega_p^2}{\omega(\omega - j\nu_p)} \right] \quad (3)$$

$$\sigma = \frac{\epsilon_0 \omega_p^2}{(j\omega + \nu_p)} \quad (4)$$

where  $\omega$  is the angular resonance frequency of the antenna,  $\nu_p$  is the angular scattering frequency, and  $\omega_p$  is the electron plasma angular frequency for bulk material at the operating wavelength  $\lambda$ . It can be seen that as the metal conductivity decreases, the losses will increase. In this paper, the desired phase shift compensation required at each unit cell element is obtained by changing the effective permittivity of the Gold substrate through the variation of the diameters of the holes according to the theory of perforated dielectric material [22].

### 3. NUMERICAL RESULTS

#### 3.1. The Unit-cell

The detailed construction of the proposed perforated nanoantenna reflectarray unit cell element is shown in Fig. 1. The antenna was designed to operate at 735 THz. The proposed square unit cell has length  $L = 600$  nm, height  $h = 70$  nm, with four identical circular holes of equal radii, and perforation depth  $d = 35$  nm. The unit cell is constructed from Silver substrate with its material properties are introduced using the Drude model. The Silver angular scattering frequency  $\nu_p$  is ( $4.35 \times 10^{12}$  rad/sec) and the electron plasma angular frequency  $\omega_p$  is ( $1.3665 \times 10^{16}$  rad/sec) at the operating wavelength of  $\lambda = 408$  nm.

To calculate the required reflection coefficient phase compensation in each unit cell, the unit cell is placed in a waveguide simulator [5]. The perfect electric and magnetic wall boundary conditions are applied to the sides of the surrounding waveguide, and result in image planes

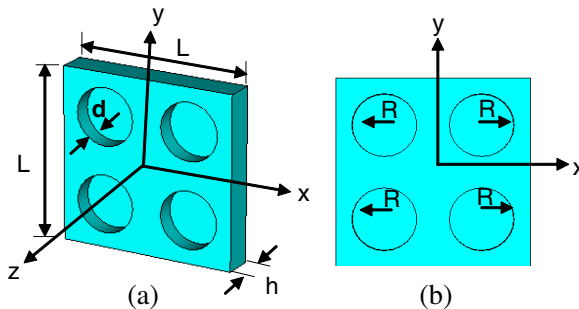


**Figure 1.** The detailed construction of the perforated reflectarray nanoantenna unit cell. (a) 3-D view. (b) Side view.

on all sides of the unit cell to represent an infinite array approximation. A linearly polarized plane wave was used as the excitation of the unit cells inside the waveguide simulator and only normal incidence angle was considered. There are several limitations to the infinite array approach. *First*, all elements of the reflectarray are identical; this is clearly not the case in the real reflectarray in which the diameters of the holes in each cell element must vary according to the required phase compensation. *Secondly*, the reflectarray itself is not infinite in extent. The separation between the holes and the number of holes are optimized to maximize the reflection from the structure as shown in Fig. 2(a). The variation of the reflection coefficient phase versus the

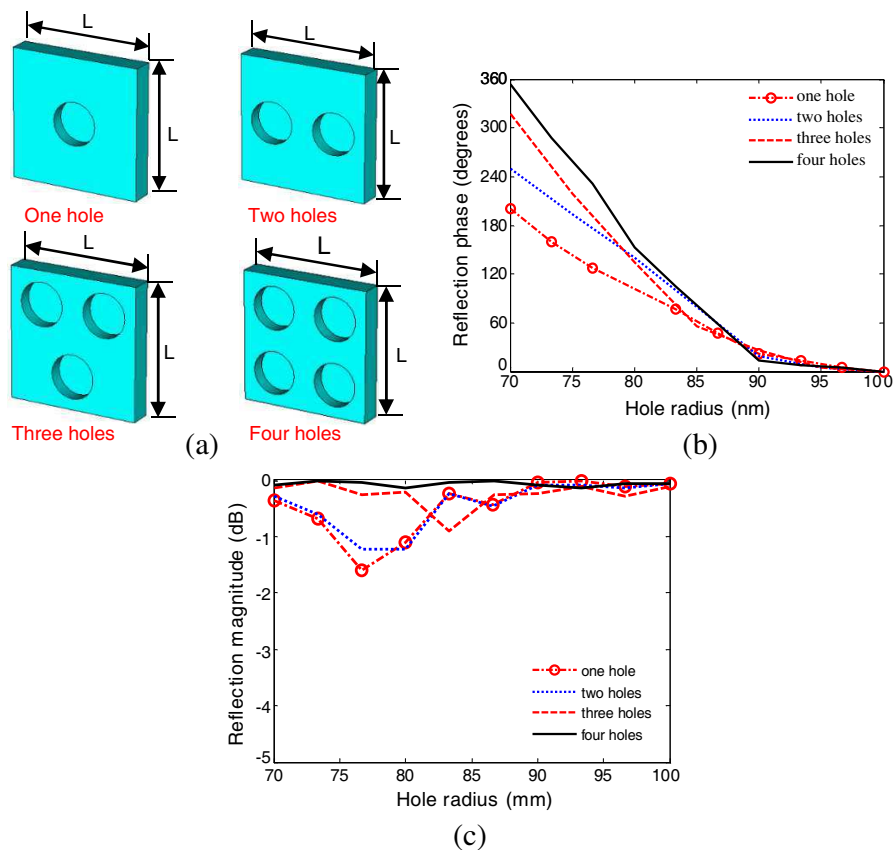


**Figure 2.** The variation of the reflection coefficient phase variation of the unit cell with different number of perforated holes. (a) The unit cell with different number of holes. (b) The reflection coefficient phase. (c) The reflection coefficient magnitude variation.

hole radius for one, two, three and four holes at 735 THz is determined using the FIT technique and is shown in Fig. 2(b). The unit cell having only one hole produce a phase shift ranging from  $0^\circ$  to about  $200^\circ$ , by increasing the number of the holes the reflection coefficient phase is increased. The unit cell having two holes achieves phase of  $250^\circ$ , unit cell with three holes achieves  $300^\circ$ , and finally the unit cell having four holes achieves  $360^\circ$  reflection coefficient phase variation. The noticed variation of the reflection coefficient phase is due to the variation of the effective dielectric constant of the Silver material. Fig. 2(c) shows the variation of the magnitude of the reflection coefficient in dBs for unit cell with different number of perforated holes. The magnitude of the reflection coefficient of the unit cell having only one-hole changes from  $-1.9$  dB to  $0$  dB. By increasing the number of holes in the unit cell, the magnitude of the reflection coefficient is increased. The unit cell having two holes achieves reflection coefficient magnitude variation from  $-1.3$  dB to  $0$  dB, unit cell with three holes achieves reflection coefficient magnitude variation from  $-1$  dB to  $0$  dB, and finally the unit cell having four holes achieves reflection coefficient magnitude variation from  $-0.2$  dB to  $0$  dB.

### 3.2. Nano-horn Antenna

Different nano-horn antennas made from nano-materials operating at THz range are investigated in [23, 24]. A linearly polarized pyramidal nano-horn antenna is used to feed the perforated nanoantenna reflectarray. The nano-horn was positioned such that the array was prime-focus fed. The nano-horn antenna is constructed from Gold substrate with its material properties introduced using the Drude model. The Gold angular scattering frequency  $\nu_p$  is ( $1.2566 \times 10^{13}$  rad/sec) and the electron plasma angular frequency  $\omega_p$  is ( $1.2566 \times 10^{16}$  rad/sec) at the operating wavelength of  $\lambda = 408$  nm. The feed nano-horn was  $L_h = 1080$  nm long, with an aperture size  $b \times a$  of  $1700$  nm  $\times$   $850$  nm as shown in Fig. 3(a). The 3-D radiation pattern from the nano-horn antenna at 735 THz is shown in Fig. 3(b). The nano-horn antenna has a gain of  $11.7$  dB at 735 THz. The radiation patterns for the pyramidal nano-horn antenna in  $E$ -plane and  $H$ -plane are shown in Fig. 4 at 735 THz. The first sidelobe levels (SLL) in the  $E$ - and  $H$ -planes are approximately  $-18.95$  dB and  $-18.86$  dB below the main peaks, respectively.

### 3.3. $9 \times 9$ Nanoantenna Reflectarray

A schematic of the perforated nanoantenna reflectarray showing the feed is shown in Fig. 5.  $9 \times 9$  unit cell elements are used to construct

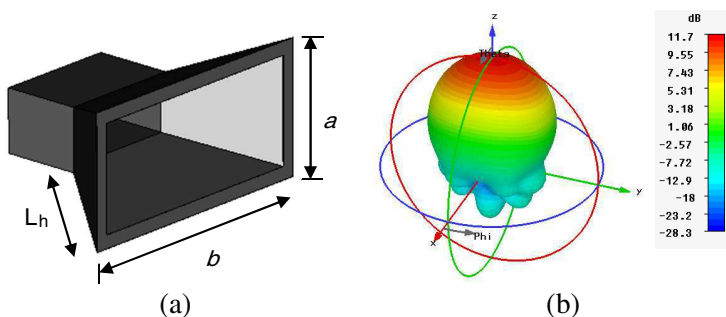


**Figure 3.** The detailed construction of the feeding horn and the 3-D gain radiation pattern at  $f = 735$  THz. (a) 3-D view of horn antenna. (b) 3-D gain pattern.

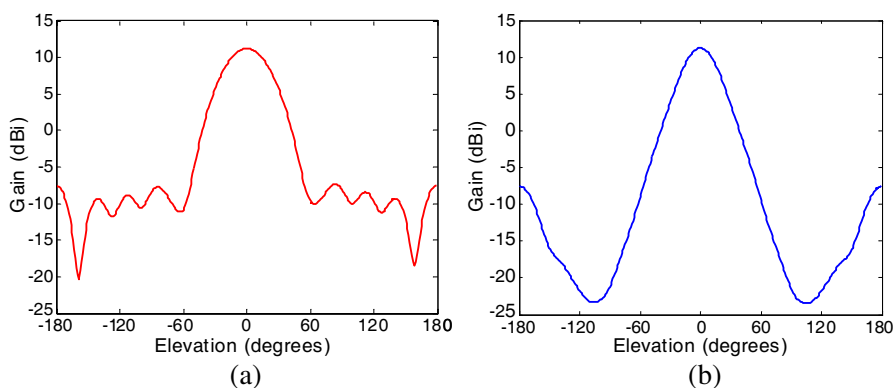


**Figure 4.** The normalized gain radiation patterns of the feeding horn antenna in different planes at 735 THz. (a)  $E$ -plane. (b)  $H$ -plane.

the array. The element spacing between the unit cells is 600 nm. The reflectarray has total dimensions of  $5400 \times 5400 \text{ nm}^2$  located in the  $x$ - $y$  plane. The perforated nanoantenna reflectarray is symmetrical about the  $x$ -axis and  $y$ -axis. The feeding horn is located at a distance  $F = 5400 \text{ nm}$  ( $F/D = 1$ ) in the normal direction of the array plane. Table 1 describes the phase shift and the corresponding hole radii relevant to the unit cells of the first quadrant of the array. The  $E$  and  $H$ -plane radiation patterns at 735 THz of the perforated nanoantenna reflectarray are shown in Fig. 6. The first SLL is 10.34 dB and 8.9 dB in  $E$ -plane and  $H$ -plane respectively. The HPBW of the reflectarray is 4 degrees in  $E$ -plane and 5.7 degrees in  $H$ -plane. The 3-D radiation pattern of the reflectarray at  $f = 735$  THz is shown in Fig. 7(a). The perforated nanoantenna reflectarray has a gain of 20.5 dB at 735 THz. Most of the radiated field is reflected through

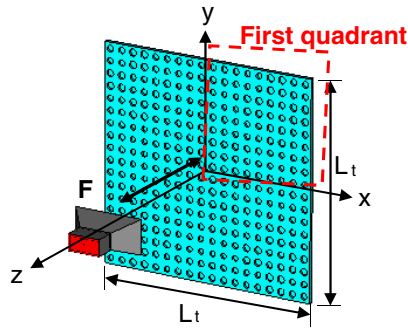


**Figure 5.** The detailed 3-D construction of the  $9 \times 9$  perforated nanoantenna reflectarray.

**Table 1.** The phase shift and the corresponding hole radii relevant to the unit cells of the first quadrant of the array.

50.4°	79.51°	165.79°	306.27°	136.55°
88.03 nm	87.1 nm	79.36 nm	72.33 nm	80.87 nm
79.5°	108.44°	194.21°	333.9°	163.17°
87.1 nm	82.99 nm	78.21 nm	70.97 nm	79.45 nm
165.79°	194.21°	278.50°	55.88°	242.21°
79.36 nm	78.21 nm	73.86 nm	87.93 nm	76.11 nm
306.27°	333.9°	55.88°	189.65°	11.38°
72.33 nm	70.97 nm	87.93 nm	78.39 nm	91.14 nm
136.55°	163.17°	242.21°	11.38°	187.2°
80.87 nm	79.45 nm	76.11 nm	91.14 nm	78.47 nm

the perforated nanoantenna reflectarray and the back lobe is due to the variation of the conductivity of the reflectarray material. The perforated nanoantenna reflectarray gain variation as a function of frequency is shown in Fig. 7(b).

The gain is varied from 14.5 dB to 20.5 dB over the frequency range with 1 dB gain variations bandwidth (6.5 THz). Theoretical radiation patterns are shown in Fig. 8 at different frequencies to check the bandwidth of the array. At the extreme frequencies, the radiation patterns are similar, with some increase in sidelobe levels. A solid Silver sheet with the same dimensions of the proposed  $9 \times 9$  perforated nanoantenna reflectarray ( $5400 \times 5400 \text{ nm}^2$ ) but with no holes is shown in Fig. 9. The solid array is fed with the same nano-horn antenna placed at a distance  $F = D$  as that in Fig. 5. The radiation patterns

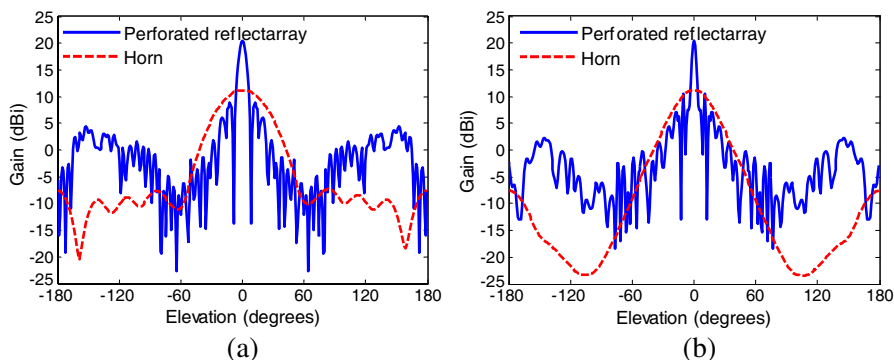


**Figure 6.** The gain patterns plot for a  $9 \times 9$  center-feed center-beam perforated nanoantenna reflectarray at 735 THz. (a) *E*-plane. (b) *H*-plane.

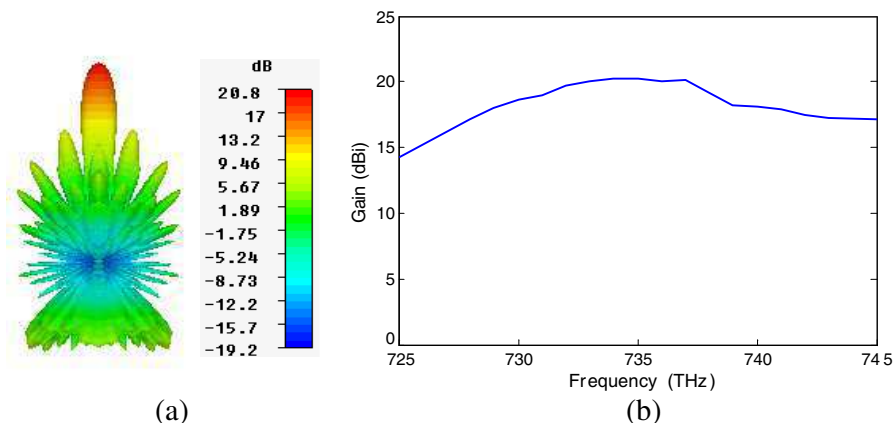


**Figure 7.** The 3-D gain radiation pattern at  $f = 735$  THz and the gain variation versus frequency and for a  $9 \times 9$  perforated nanoantenna reflectarray. (a) 3-D gain pattern at  $f = 735$  THz. (b) The gain variation versus frequency.

from the solid sheet from Silver material (with no holes) with the same size of the nanoantenna reflectarray are shown in Fig. 10. The gain of the solid Silver sheet is almost a copy of the gain of the horn except that the side lobes are a little stronger. This is because the solid Silver sheet has a finite size. It is quite likely that the side lobes are Airy features (diffraction limit) since the calculated area of the sheet is only about 12 wavelengths in size. The nano-horn antenna in front of the solid sheet blocks a part of the reflected beam and reduce the main beam. The gain variation versus frequency of the solid sheet is illustrated in

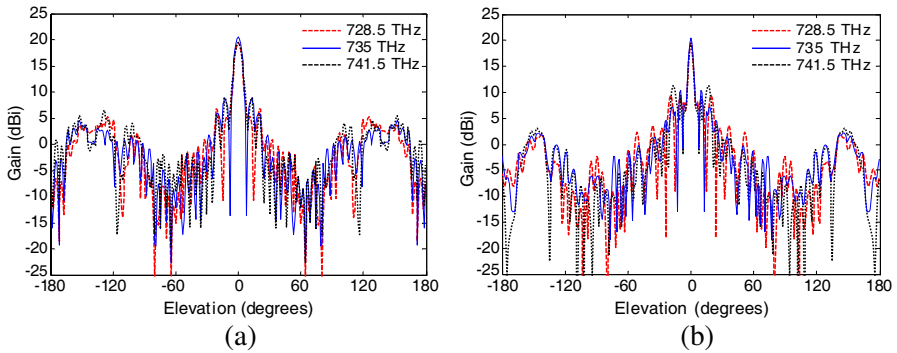


**Figure 8.** The gain radiation patterns plot for a  $9 \times 9$  center-feed center-beam perforated nanoantenna reflectarray at different frequencies. (a)  $E$ -plane. (b)  $H$ -plane.

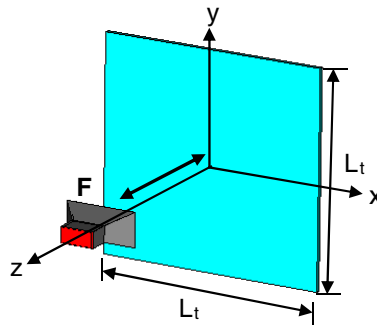


**Figure 9.** The detailed 3-D construction of the solid Silver sheet.

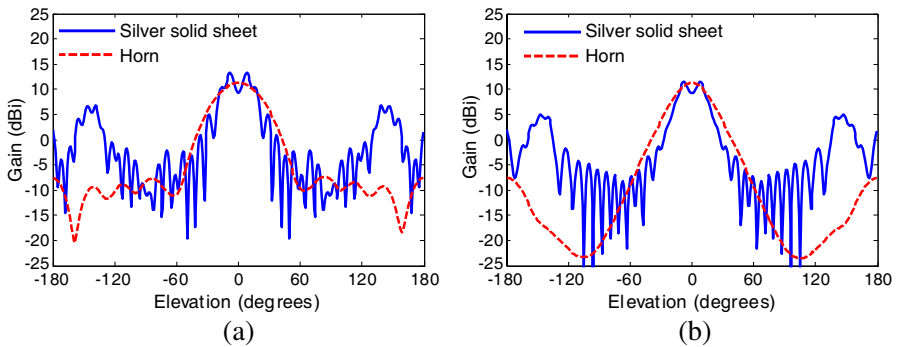


**Figure 10.** The gain radiation patterns plot for a solid Silver sheet at  $f = 735$  THz. (a)  $E$ -plane. (b)  $H$ -plane.

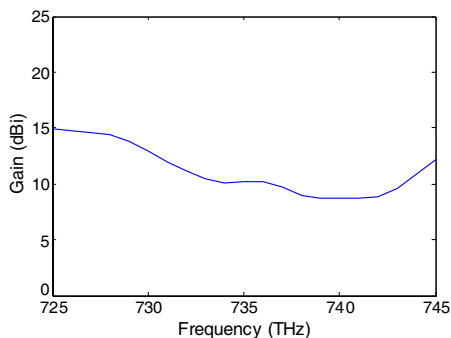


**Figure 11.** The gain variation versus frequency for a solid Silver sheet.

Fig. 11. Due to the lack of phase compensation in the solid surface, the gain is much less than the free space horn antenna gain. In the solid surface, there is no transformation of the spherical wave into a plane wave.

#### 4. CONCLUSION

In this paper, a design of perforated nanoantenna reflectarray is investigated. A perforated Silver material is used to construct the array unit cell. The number of the perforation holes is optimized in order to obtain reflection coefficient phase variation from  $0^\circ$  to  $360^\circ$  with maximum reflection magnitude ( $\sim 1$ ). The radiation characteristics of linearly polarized pyramidal nano-horn antenna are investigated. The nano-horn antenna has a gain of 11.7 dB at 735 THz. The first side lobe levels (SLL) in the  $E$ - and  $H$ -planes are approximately  $-18.95$  dB and  $-18.86$  dB below the main peaks respectively. Using the proposed unit cell a  $9 \times 9$  perforated nanoantenna reflectarray is designed. The first SLL is 10.34 dB and 8.9 dB in  $E$ -plane and  $H$ -plane respectively. The HPBW of the reflectarray is 4 degrees in  $E$ -plane and 5.7 degrees in  $H$ -plane. The gain is varied from 14.5 dB to 20.5 dB over the frequency range with 1 dB gain variations bandwidth (6.5 THz). A comparison between solid Silver sheet and a perforated nanoantenna reflectarray shows that the variation of the perforation hole radius better compensate the phase of the spherical wave to be transformed into a plane wave and thus improves the reflectarray gain.

#### REFERENCES

1. Huang, J. and J. A. Encinar, *Reflectarray Antennas*, John Wiley and Sons, Inc., Hoboken, NJ, USA, 2007.

2. Hansen, R. C., *Phased Array Antennas*, John Wiley & Sons, 1998.
3. Dzulkipli, I., M. H. Jamaluddin, R. Ngah, M. R. B. Kamarudin, N. Seman, and M. K. Abd Rahim, "Mutual coupling analysis using FDTD for dielectric resonator antenna reflectarray radiation prediction," *Progress In Electromagnetics Research B*, Vol. 41, 121–136, 2012.
4. Jamaluddin, M. H., R. Sauleau, X. Castel, R. Benzerger, L. Le Coq, R. Gillard, and T. Koleck, "Design, fabrication and characterization of a dielectric resonator antenna reflectarray in Ka-band," *Progress In Electromagnetics Research B*, Vol. 25, 261–275, 2010.
5. Zainud-Deen, S. H., E. Abd, A. A. Mitkees, and A. A. Kishk, "Design of dielectric resonator reflectarray using full-wave analysis," *National Radio Science Conference (NRSC 2009)*, 1–9, Egypt, 2009.
6. Cadoret, D., L. Marnat, R. Loison, R. Gillard, H. Legay, and B. Salome, "A dual linear polarized printed reflectarray using slot loaded patch elements," *The 2nd European Conference Antenna and Propagation (EUCAP 2007)*, 1–5, 2007.
7. Radi, Y., S. Nikmehr, and A. Pourziad, "A novel bandwidth enhancement technique for X-band RF MEMS actuated reconfigurable reflectarray," *Progress In Electromagnetics Research*, Vol. 111, 179–196, 2011.
8. Rengarajan, S. R., "Reflectarrays of rectangular microstrip patches for dual-polarization dual-beam radar interferometers," *Progress In Electromagnetics Research*, Vol. 133, 1–15, 2013.
9. Novotny, L. and N. van Hulst, "Antennas for light," *Nature Photonics*, Vol. 5, 83–90, February 2011.
10. Novotny, L. and B. Hecht, *Principles of Nano-optics*, Cambridge University Press, New York, USA, 2006.
11. Miroshnichenko, A. E., I. S. Maksymov, R. Davoyan, C. Simovski, P. Belov, and Y. S. Kivshar, "An arrayed nanoantenna for broadband light emission and detection," *Physica Status Solidi (RRL)-rapid Research Letters*, Vol. 5, No. 9, 347–349, September 2011.
12. Stockman, M. I., "Nanofocusing of optical energy in tapered plasmonic waveguides," *Physical Review Letters*, Vol. 93, No. 13, 7404–7408, 2004.
13. Atwater, H. A. and A. Polman, "Plasmonics for improved photovoltaic devices," *Nature Material*, Vol. 9, 205–213, September 2010.

14. Liu, N., M. L. Tang, M. Hentschel, H. Giessen, and A. P. Alivisatos, "Nanoantenna-enhanced gas sensing in a single tailored nanofocus," *Nature Material*, Vol. 10, 631–636, May 2011.
15. De Angelis, F., G. Das, P. Candeloro, M. Patrini, M. Galli, A. Bek, M. Lazzarino, I. Maksymov, C. Liberale, L. C. Andreani, and E. di Fabrizio, "Nanoscale chemical mapping using three-dimensional adiabatic compression of surface plasmon polaritons," *Nature Nanotechnology*, Vol. 5, 67–72, November 2010.
16. Maksymov, I. S., M. Besbes, J. P. Hugonin, J. Yang, A. Beveratos, I. Sagnes, I. Robert-Philip, and P. Lalanne, "Metal-coated nanocylinder cavity for broadband nonclassical light emission," *Physical Review Letters*, Vol. 105, No. 18, 502–506, 2010.
17. Al'u, A. and N. Engheta, "Wireless at the nanoscale: Optical interconnects using matched nanoantennas," *Physical Review Letters*, Vol. 104, No. 21, 3902–3906, 2010.
18. Ahmadi, A., "Metamaterials demonstrating focusing and radiation characteristics applications," Ph.D. Thesis, The Field of Electrical Engineering, Northeastern University, Boston, Massachusetts, August 2010.
19. Chair, R., A. A. Kishk, and K. F. Lee, "Experimental investigation for wideband perforated dielectric resonator antenna," *Electronic Letters*, Vol. 42, No. 3, 137–139, February 2006.
20. Cooke, S. J., R. Shtokhamer, A. A. Mondelli, and B. Levush, "A finite integration method for conformal, structured-grid, electromagnetic simulation," *Journal of Computational Physics*, Vol. 215, 321–347, 2006.
21. Özbay, E., "Plasmonics: Merging photonics and electronics at nanoscale dimensions," *Science Magazine*, Vol. 311, No. 5758, 189–193, January 2006.
22. Zhang, Y. and A. A. Kishk, "Analysis of dielectric resonator antenna arrays with supporting perforated rods," *2nd European Conf. on Antennas and Propag., (EuCAP 2007)*, 1–5, 2007.
23. Ramaccia, D., F. Bilotti, A. Toscano, and A. Massaro, "Efficient and wideband horn nanoantenna," *Optics Letters*, Vol. 36, No. 10, 1743–1745, May 2011.
24. Ramaccia, D., F. Bilotti, A. Toscano, R. Cingolani, and A. Massaro, "Electrical and radiation properties of a horn nanoantenna at near infrared frequencies," *Proc. of IEEE (AP-S/URSI)*, 2407–2410, 2011.